



CADM1 associates with Hippo pathway core kinases; membranous co-expression of CADM1 and LATS2 in lung tumors predicts good prognosis

Takeshi Ito¹ | Atsuko Nakamura¹ | Ichidai Tanaka² | Yumi Tsuboi¹ | Teppei Morikawa³ | Jun Nakajima⁴ | Daiya Takai⁵ | Masashi Fukayama³ | Yoshitaka Sekido⁶ | Toshiro Niki⁷ | Daisuke Matsubara^{1,7}  | Yoshinori Murakami¹ 

¹Molecular Pathology Laboratory, Institute of Medical Science, The University of Tokyo, Tokyo, Japan

²Department of Respiratory Medicine, Nagoya University Graduate School of Medicine, Aichi, Japan

³Human Pathology Department, Graduate School of Medicine, The University of Tokyo, Tokyo, Japan

⁴Department of Thoracic Surgery, The University of Tokyo, Tokyo, Japan

⁵Department of Respiratory Medicine, Graduate School of Medicine, The University of Tokyo, Tokyo, Japan

⁶Division of Molecular Oncology, Aichi Cancer Center Research Institute, Aichi, Japan

⁷Division of Integrative Pathology, Jichi Medical University, Tochigi, Japan

Correspondence

Daisuke Matsubara, Division of Integrative Pathology, Jichi Medical University, Yakushiji, Shimotsukeshi, Tochigi, Japan. Email: VZV07574@nifty.com

Funding information

Japan Society for the Promotion of Science, Grant/Award Number: 16K08672, 16K18142, 18H02634, 25290051, 25460432 and 26293080; Research on Human Genome Tailor-made from the Ministry of Health, Labor, and Welfare of Japan; the Foundation for the Development of the Community

Abstract

Cell adhesion molecule-1 (CADM1) is a member of the immunoglobulin superfamily that functions as a tumor suppressor of lung tumors. We herein demonstrated that CADM1 interacts with Hippo pathway core kinases and enhances the phosphorylation of YAP1, and also that the membranous co-expression of CADM1 and LATS2 predicts a favorable prognosis in lung adenocarcinoma. CADM1 significantly repressed the saturation density elevated by YAP1 overexpression in NIH3T3 cells. CADM1 significantly promoted YAP1 phosphorylation on Ser 127 and downregulated YAP1 target gene expression at confluency in lung adenocarcinoma cell lines. Moreover, CADM1 was co-precipitated with multiple Hippo pathway components, including the core kinases MST1/2 and LATS1/2, suggesting the involvement of CADM1 in the regulation of the Hippo pathway through cell-cell contact. An immunohistochemical analysis of primary lung adenocarcinomas (n = 145) revealed that the histologically low-grade subtype frequently showed the membranous co-expression of CADM1 (20/22, 91% of low-grade; 61/91, 67% of intermediate grade; and 13/32, 41% of high-grade subtypes; $P < 0.0001$) and LATS2 (22/22, 100% of low-grade; 44/91, 48% of intermediate-grade; and 1/32, 3% of high-grade subtypes; $P < 0.0001$). A subset analysis of disease-free survival revealed that the membranous co-expression of CADM1 and LATS2 was a favorable prognosis factor (5-year disease-free survival rate: 83.8%), even with nuclear YAP1-positive expression (5-year disease-free survival rate: 83.7%), whereas nuclear YAP1-positive cases with the negative expression of CADM1 and LATS2 had a poorer prognosis (5-year disease-free survival rate: 33.3%). These results indicate that the relationship between CADM1 and Hippo pathway core kinases at the cell membrane is important for suppressing the oncogenic role of YAP1.

Ito and Nakamura contributed equally to this work.

Matsubara and Murakami are co-last authors.

This is an open access article under the terms of the Creative Commons Attribution-NonCommercial-NoDerivs License, which permits use and distribution in any medium, provided the original work is properly cited, the use is non-commercial and no modifications or adaptations are made.

© 2019 The Authors. *Cancer Science* published by John Wiley & Sons Australia, Ltd on behalf of Japanese Cancer Association.

KEY WORDS

CADM1, Hippo pathway, LATS2, lung adenocarcinoma, YAP1

1 | INTRODUCTION

Lung cancer is the leading cause of cancer death in many developed countries, including the United States and Japan,^{1,2} and adenocarcinoma is the most common histological subtype of primary lung cancer.

The loss or inactivation of various tumor suppressor genes has been implicated in the development of lung adenocarcinoma, and the chromosome 11q23-encoded gene, *CADM1* (cell adhesion molecule-1), was identified as a critical tumor suppressor by its inhibitory effects on tumor formation in human lung adenocarcinoma cell lines.^{3,4}

Cell adhesion molecule-1 is a member of the immunoglobulin superfamily of cell adhesion molecules (IgCAM). *CADM1* is expressed at the lateral membrane in normal epithelial cells, and mediates cell-cell attachment by binding with *CADM1* expressed in adjacent cells.⁵ *CADM1* expression is frequently lost or reduced in concordance with tumor progression; lepidic growth components were positive for *CADM1* expression, while invasive components of the same tumors were frequently negative for *CADM1* in lung adenocarcinoma.⁶ Mao et al⁷ reported that high expression levels of *CADM1* inhibited cell proliferation and induced apoptosis in lung adenocarcinoma cell lines. The cytoplasmic domain of *CADM1* is an important region for conserving the tumor suppressive function of *CADM1*.⁸ However, the mechanisms underlying the anti-proliferative and pro-apoptotic activities of *CADM1* have not yet been elucidated in detail.

It has recently become increasingly apparent that abnormalities in upstream and downstream members of the Hippo pathway, which have been implicated in the cell contact inhibition of proliferation as well as organ size control, play important roles in the tumorigenesis of various human cancers.⁹ YAP1 is the main downstream effector of the Hippo pathway that promotes cell growth as a transcription cofactor and may be inactivated through its phosphorylation by the upstream kinases LATS1/2.¹⁰

In *Drosophila*, Echinoid, an IgCAM member, was shown to function as an upstream regulator of the Hippo pathway. The loss of Echinoid compromises the phosphorylation of Yorkie (YAP1 in mammals), resulting in elevated Yorkie activity that drives tissue overgrowth.¹¹

In the present study, we showed that *CADM1* associates with the Hippo pathway core kinases, MST1/2 and LATS1/2, and may increase the phosphorylation of YAP1 through cell-cell contact. We also demonstrated, through an immunohistochemical analysis, that LATS2 was significantly co-expressed with *CADM1* in the membranes of primary lung adenocarcinomas, and that the membranous co-expression of *CADM1* and LATS2 correlated with a better prognosis. This is the first study to show that *CADM1* is involved in the regulation of the Hippo signaling pathway through cell-cell contact.

2 | MATERIALS AND METHODS

2.1 | Cell lines

The human lung adenocarcinoma cell line HCC827 was obtained from the RIKEN BioResource Center (Tsukuba, Japan) and the NCI-H292 and NCI-H1838 cell lines were from the ATCC (Manassas, VA, USA). The mouse fibroblast cell line NIH3T3 was obtained from the ATCC. The human embryonic kidney cell line 293FT was purchased from Thermo Fisher Scientific (Waltham, MA, USA). The Plat-A retroviral packaging cell line was a kind gift from Dr Toshio Kitamura (Institute of Medical Science, University of Tokyo). HCC827, NCI-H292 and NCI-H1838 cells were cultured in RPMI 1640 (Nacalai Tesque, Kyoto, Japan) supplemented with 10% FBS (Biowest, Nuaille, France), 100 units/mL penicillin and 100 µg/mL streptomycin (Sigma-Aldrich, St. Louis, MO, USA). NIH3T3 and 293FT cells were cultured in DMEM (Nacalai Tesque) supplemented with 10% FBS, 100 units/mL penicillin and 100 µg/mL streptomycin. Plat-A cells were cultured in DMEM with 4.5 g/L glucose supplemented with 10% FBS, 100 units/mL penicillin, 100 µg/mL streptomycin, 1 µg/mL puromycin (Wako Pure Chemical Industries, Tokyo, Japan) and 10 µg/mL blasticidin (Kaken Pharmaceutical, Tokyo, Japan). Cells were maintained at 37°C in a humidified 5% CO₂ incubator (Panasonic, Osaka, Japan).

2.2 | Antibodies for Western blotting

Rabbit monoclonal anti-LATS1 (C66B5), anti-phospho-LATS1 (Thr1079) (D57D3), anti-phospho-YAP1 (Ser397) (D1E7Y) and anti-YAP (D8H1X) antibodies and a rabbit polyclonal anti-phospho-YAP (Ser127) antibody were purchased from Cell Signaling Technology (Danvers, MA, USA). Rabbit polyclonal anti-LATS2 antibodies were obtained from Novus Biologicals (Centennial, CO, USA) and Atlas Antibodies (Bromma, Sweden). The rabbit polyclonal anti-*CADM1* (C-18) antibody was previously described.¹² Goat polyclonal anti-GAPDH (V-18), rat monoclonal anti-HA (3F10) and mouse monoclonal anti-V5 (E10/V4RR) antibodies were purchased from Santa Cruz Biotechnology (Dallas, TX, USA), Roche (Basel, Switzerland) and Thermo Fisher Scientific, respectively.

2.3 | Western blotting

Cell lysates were extracted using RIPA buffer (50 mmol/L Tris-HCl [pH 7.5], 150 mmol/L NaCl, 1 mmol/L EDTA, .1% SDS and .5% sodium deoxycholate) containing a protease inhibitor cocktail (200 µmol/L AEBSF, 10 µmol/L leupeptin and 1 µmol/L pepstatin A) and phosphatase inhibitor cocktail (10 mmol/L NaF and 1 mmol/L Na₃VO₄). Protein samples were prepared by mixing lysates with 4 × sample

buffer (.25 mol/L Tris-HCl [pH 6.8], 40% glycerol, 8% SDS, 20% 2-mercaptoethanol and .02% bromophenol blue) and then boiling at 95°C for 5 minutes. Equal amounts of total protein were fractionated in 5%-10% SDS-PAGE, transferred to a polyvinylidene difluoride membrane (Merck Millipore, Burlington, VT, USA), and incubated with primary antibodies in Can Get Signal Immunoreaction Enhancer Solution (Toyobo, Osaka, Japan). Primary antibody binding was detected using the Pierce Western Blotting Substrate (Thermo Fisher Scientific) with HRP-conjugated secondary antibodies (GE Healthcare, Chicago, IL, USA). Signals were visualized using ImageQuant LAS 4000 Mini (GE Healthcare) and quantified with ImageJ software.

2.4 | Retroviral gene transfer

The Ig κ secretion leader sequence followed by *CADM1* lacking its signal peptide sequence (45-442 a.a.) with an N-terminal HA tag (HA-CADM1) was cloned into the *EcoRI-SalI* site of a pBabe-puro vector, which was a gift from Drs Hartmut Land, Jay Morgenstern and Bob Weinberg (Addgene plasmid #1764).¹³ *YAP1* was cloned into the *EcoRI-NotI* site of a pMX-IRES-GFP vector.¹⁴ Retroviral vectors were then transfected into Plat-A cells using Lipofectamine LTX (Thermo Fisher Scientific). After 48 hours, NIH3T3 cells were infected with the retrovirus by incubating with the culture supernatant of Plat-A cells. *CADM1*-expressing cells were obtained by puromycin selection at a concentration of 10 μ g/mL. *YAP1*-expressing cells were obtained by sorting GFP-positive cells with FACS Aria II (BD Biosciences, Franklin Lakes, NJ, USA).

2.5 | Lentiviral gene transfer

HA-CADM1 was cloned in a pENTR/D-TOPO vector (Thermo Fisher Scientific). The lentiviral expression vector was then obtained by Gateway recombination with pLenti6-V5/DEST (Thermo Fisher Scientific). The vector obtained and ViraPower Lentiviral Packaging Mix (Thermo Fisher Scientific) were co-transfected into 293FT cells using Polyethylenimine Max (Polysciences, Warrington, UK). After 48 hours, HCC827 cells were infected with the lentivirus by incubating with the culture supernatant of 293FT cells containing 5 μ g/mL Polybrene (Nacalai Tesque). HCC827 cells expressing HA-CADM1 were selected by 20 μ g/mL blasticidin.

2.6 | Immunoprecipitation

The coding sequences of *WWC1/KIBRA*, *LATS1*, *LATS2*, *MST1*, *MST2*, *SAV1*, *YAP1* and *YWHAH/14-3-3 η* without stop codons were cloned into the pENTR/D-TOPO vector. The templates used for cloning are listed in Table S1. Gateway Entry clones of the *AMOT* (100073116), *AMOTL1* (100002205) and *NF2* (100009338) genes without stop codons were purchased from DNAFORM (Yokohama, Japan). Expression vectors were obtained by Gateway recombination with a pHEK-V5 destination vector, which was generated by replacing the human IgG2-Fc fragment of the pHEK-Fc vector¹⁵ with the V5 peptide sequence. Expression vectors and a pHEK293 Enhancer Vector

(Takara Bio, Kusatsu, Japan) were transfected into 293FT cells using Polyethylenimine Max in 10-cm dishes. After 24 hours, cells were collected and lysed with lysis buffer (25 mmol/L Tris-HCl [pH 7.5], 150 mmol/L NaCl, 1% NP-40, 1 mmol/L EDTA and 5% glycerol) containing protease and phosphatase inhibitor cocktails. Lysates were centrifuged at 20,600 g at 4°C for 10 minutes, supernatants were pre-cleared with normal rabbit IgG (R&D Systems) and protein A-sepharose (GE Healthcare) at 4°C for 1 hour, and then incubated with the antibody against *CADM1* or normal rabbit IgG at 4°C overnight. After incubating with protein A-sepharose at 4°C for 2 hours, sepharose was washed 4 times with lysis buffer, suspended in a sample buffer, boiled at 95°C for 5 minutes, and then incubated on ice. Samples were then subjected to SDS-PAGE followed by western blotting.

2.7 | Real-time quantitative PCR

Total RNA was extracted using an RNeasy Mini Kit (Qiagen, Hilden, Germany) from cells collected 3 days after seeding at 1×10^6 cells on a 6-cm dish. First-strand cDNA was synthesized using the ReverTra Ace qPCR RT Kit (Toyobo). Real-time PCR was performed using the ABI 7300 Real-Time PCR System (Applied Biosystems, Waltham, MA, USA) with the SYBR Green PCR Master Mix (Applied Biosystems). Relative gene expression was calculated using the *ddCt* method. The sequences of primers used to detect gene expression were as follows: for *ANKRD1*, sense 5'-AAGCAGGAGGATCTGAAGACACTT-3' and antisense 5'-GTTGTTTCTCGCTTTTCCACTGT-3'; for *CYR61*, sense 5'-GCGTTTCCCTTCTACAGGCT-3' and antisense 5'-TTCTCCAATCGTGCTGCAT-3'; for *GAPDH*, sense 5'-CAACGGATTGGTCGTATTGG-3' and antisense 5'-GCAACAATATCCACTTTACCAGAGTTAA-3'.

2.8 | Tissue microarrays

We used 7 different tissue microarrays (TMAs) that were produced to accommodate primary lung adenocarcinoma tissue core sections collected from patients ($n = 166$) who had undergone surgical resection at the University of Tokyo Hospital between June 2005 and September 2008. Core sections were carefully selected from histologically predominant invasive components in the case of adenocarcinoma with mixed subtypes by pathologists in the Department of Pathology, the University of Tokyo. Informed consent was obtained from all patients, and the study was approved by the Institutional Ethics Review Committee. Of 166 core sections, 12 were missing from TMA sections, and only 9 invasive adenocarcinoma cases (except minimally invasive adenocarcinoma cases) showed lepidic growth components without invasive lesions on TMA sections because of repeated slicing; therefore, the immunohistochemical analysis was performed using the data of 145 cases. Patients ($n = 145$) included 78 men and 67 women, ranging in age between 34 and 86 years (average 66.2 years). Each case was reassigned for its TNM classification and pathological stage based on the 7th Edition of the TNM Classification for Lung Cancer¹⁶: 18 were Stage 0, 89 Stage I (43 Stage IA, 46 Stage IB), 10 Stage II (5 Stage IIA, 5 Stage IIB), 22 Stage III (17 Stage IIIA, 5 Stage

IIIB), and 4 Stage IV. The stages of 3 cases were unknown (2 were more than Stage I). A total of 145 cases included 16 non-mucinous adenocarcinomas in situ, 9 minimally invasive adenocarcinomas and 120 invasive adenocarcinomas. Each case was classified by 2 pathologists (D. M. and T. M.) based on the predominant histopathological subtype in the invasive lesion on TMA sections, except for cases of adenocarcinoma in situ and minimally invasive adenocarcinoma that showed lepidic growth components without invasive lesions on TMA sections, as follows: lepidic growth components (without an invasive lesion) ($n = 22$), papillary adenocarcinoma ($n = 60$), acinar adenocarcinoma ($n = 31$), solid adenocarcinoma ($n = 30$) and invasive mucinous adenocarcinoma ($n = 2$). These cases were also classified into 3 grades: low-grade containing lepidic growth ($n = 22$), intermediate-grade containing acinar and papillary adenocarcinomas ($n = 91$), and high-grade containing solid and invasive mucinous adenocarcinomas ($n = 32$), by referring to the histopathological grading described previously by Yoshizawa et al¹⁷ with a slight modification.

2.9 | Immunohistochemistry

Tissue sections for CADM1, LATS2 and YAP1 were initially treated with .3% hydrogen peroxide in methanol for 30 minutes to block endogenous peroxidase activity, and then autoclaved in 10 mmol/L citrate buffer (pH 6.0) at 120°C for 10 minutes. Sections were then preincubated with 10% normal horse serum in PBS incubated with a rabbit polyclonal anti-CADM1 (C-18) antibody at a dilution of 1:1000, a mouse monoclonal anti-human LATS2 (HPA039191) antibody from Atlas Antibodies at a dilution of 1:25, and a rabbit monoclonal anti-human YAP1 (ab52771) antibody from Abcam at a dilution of 1:200 at 4°C overnight. The CADM1 antibody was detected with the DAKO Envision System-HRP Anti-rabbit system, the LATS2 antibody was detected with the DAKO LSAB2 streptavidin-peroxidase system, and the YAP1 antibody was detected with the DAKO Envision™ + Dual Link System, according to the manufacturer's instructions. 3,3'-Diaminobenzidine tetrahydrochloride (DAB) was used as a chromogen, whereas hematoxylin was used as a light counterstain.

2.10 | Evaluation of immunohistochemistry

Immunohistochemical staining was evaluated independently by 2 pathologists (D. M. and T. M.) through light microscopic observations and without knowledge of the clinical data of each patient. Cases of disagreement were reviewed jointly to reach a consensus score.

Membranous staining was assessed for CADM1. Immunohistochemical results were subdivided into 2 categories, positive and negative, with cut-off values of 30% of tumor cells for CADM1, by referring to a previous study.⁶

Membranous and cytoplasmic staining was assessed for LATS2. Immunohistochemical results were subdivided into 2 categories, positive and negative, with cut-off values of 30% of tumor cells for LATS2. LATS2-positive cases were also divided into membrane-positive cases (with or without cytoplasmic expression) and cytoplasm-positive cases (without membranous expression).

Cytoplasmic and nuclear staining was assessed for YAP1. Immunoreactivity was evaluated semi-quantitatively based on the intensity and estimated percentage of tumor cells that were stained. Intensity was quantified as follows: 1+, weak staining (detection required a high magnification); 2+, moderate staining (readily detected at a medium magnification); 3+, strong staining (readily detected at a low magnification). The percentages of positive cells were scored into 5 categories: 0, 0%; 1, 1%-25%; 2, 26%-50%; 3, 51%-75%; 4, 76%-100%. The product of the intensity and percentage scores was used as the final staining score. Final scores for nuclear/cytoplasmic YAP1 staining were defined as negative (final staining score <5) and positive (final staining score ≥ 5).

2.11 | Statistical analysis

The χ^2 -test was used to evaluate clinicopathological correlations, except for histopathological grades. The Mann-Whitney *U*-test was used to evaluate histopathological grades, with each grade being scored as follows: low-grade 1, intermediate-grade 2, and high-grade 3. Survival curves were generated using the Kaplan-Meier method and differences in survival were analyzed using the Wilcoxon method. Results were considered to be significant if the *P*-value was <0.05. All statistical calculations were performed using the StatView computer program (Abacus Concepts).

3 | RESULTS

3.1 | CADM1 repressed the saturation density elevated by YAP1 overexpression in NIH3T3 cell lines

We compared cell growth among NIH3T3 cell lines transfected with CADM1 and YAP1 together (+CADM1/YAP1), CADM1 and the control vector pMX (+CADM1/vec), the control vector pBABE and YAP1 (+vec/YAP1), and both control vectors (+vec/vec) (Figure 1). As previously reported,¹⁸ the overexpression of YAP1 promoted cell growth and elevated the saturation density of NIH3T3 cell lines, and the saturation density elevated by YAP1 was significantly repressed by CADM1 (Figure 1B). These results suggested that CADM1 is involved in cell density sensing through cell-cell adhesion, and that the inactivation of CADM1 induces the loss of contact inhibition, leading to cancer development.

3.2 | Involvement of CADM1 in the control of contact inhibition through the Hippo pathway

We used the lung adenocarcinoma cell line HCC827 with low levels of endogenous CADM1 expression. We established HCC827 cells overexpressing CADM1 and examined the effects of CADM1 on: (i) the phosphorylation of YAP1 on Ser 127 and Ser 397; and (ii) the expression levels of YAP1 target genes.

YAP1 phosphorylation on Ser 127 correlated with its nuclear-cytoplasmic translocation, while that on Ser 397 correlated with its degradation.¹⁹

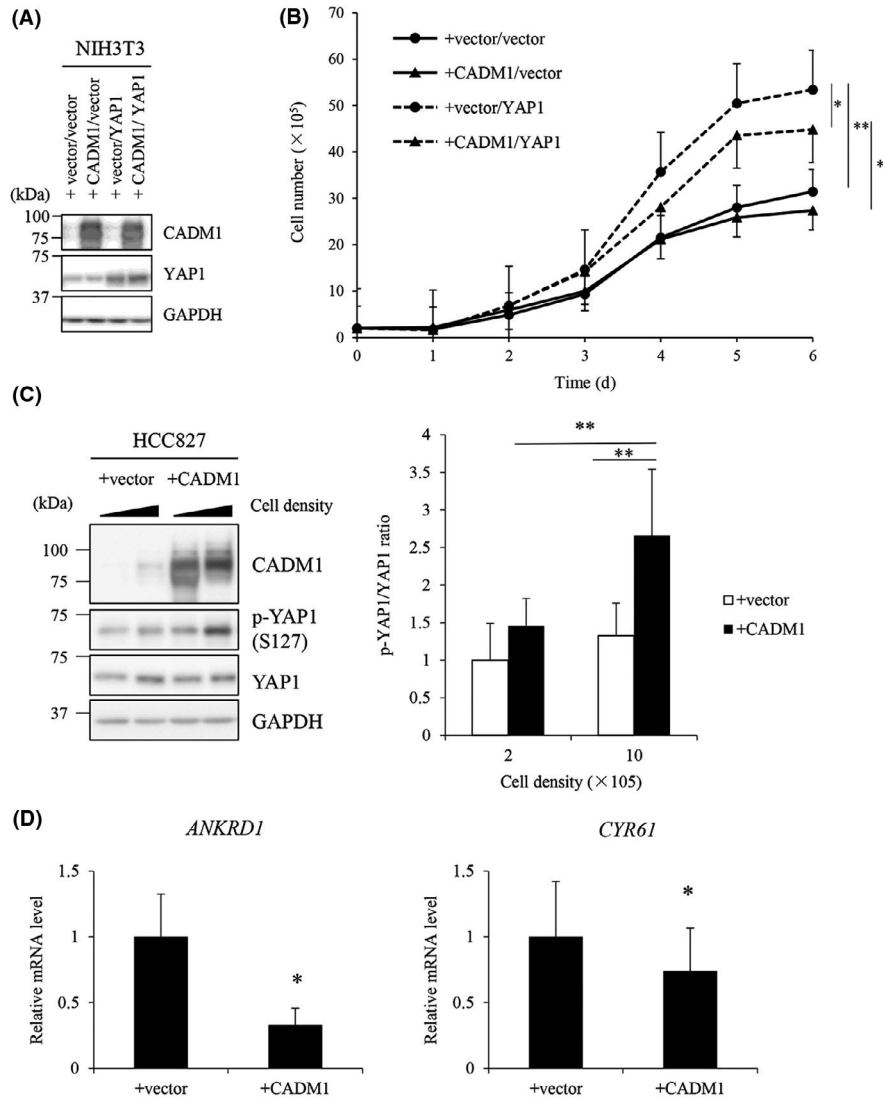


FIGURE 1 CADM1 is involved in regulating the contact inhibition of growth and phosphorylation of YAP1 in confluent cells. A, Generation of NIH3T3 cells overexpressing CADM1 and/or YAP1. The protein expression levels of CADM1, YAP1 and GAPDH in NIH3T3 cells transfected with either CADM1 or YAP1 (+CADM1/vec and +vec/YAP1), both (+CADM1/YAP1), or neither (+vec/vec) were confirmed by western blotting. B, Saturation density of NIH3T3 cells transfected with either CADM1 or YAP1, both, or neither. Cells were seeded at 2×10^5 cells on 6-cm dishes and the cell number was counted every day until day 7. Mean \pm SE of the cell number were shown ($n = 4$, $*P < 0.05$, $**P < 0.01$, paired t test). C, The phosphorylation status of YAP1 (ser 127) in HCC827 cells transfected with an empty vector (+vector) or CADM1 expression vector (+CADM1). Cells were seeded at 2×10^5 or 1×10^6 cells on 6-cm dishes and harvested after a 3-d culture. The signals of YAP1 and p-YAP1 obtained by western blotting (left) were quantified using ImageJ software. The ratio of p-YAP1/YAP1 in each cell was shown as a bar graph (mean \pm SD, $n = 7$, $**P < 0.01$, paired t test) (right). D, The mRNA expression levels of the YAP1 target genes, *ANKRD1* and *CYR61*, in HCC827 + vector and HCC827 + CADM1 cells were quantified by real-time PCR. Mean \pm SD of the relative expression were shown ($n = 4$, $*P < 0.05$, paired t test)

Under a high cell density, CADM1 significantly promoted the phosphorylation of YAP1 on Ser 127 (Figure 1C) and downregulated YAP1 target gene expression (Figure 1D) from those in the control. However, no significant difference was observed in the level of YAP1 phosphorylation on Ser 127 under a low cell density (Figure 1C). The induction of YAP1 phosphorylation on Ser 127 by CADM1 at confluence was also confirmed in a different lung adenocarcinoma cell line, NCI-H292 (Figure S1).

Figure S2 also shows no significant effect of CADM1 on the phosphorylation of YAP1 on Ser 397 regardless of cell density,

suggesting that CADM1 is not involved in the degradation of YAP1.

3.3 | Interaction between CADM1 and Hippo pathway core molecules

The regulatory mechanisms of the Hippo pathway by CADM1 have not yet been elucidated in detail; therefore, we performed immunoprecipitation assays to examine the relationship between CADM1 and Hippo pathway core molecules. The results obtained showed that CADM1

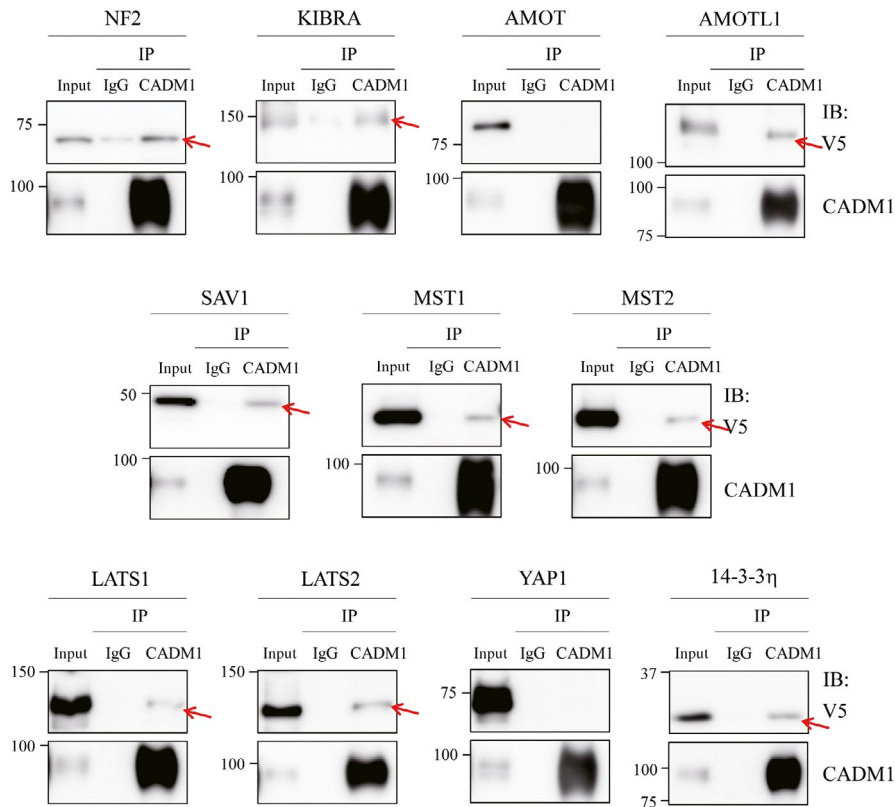


FIGURE 2 CADM1 interacts with multiple Hippo pathway components; 293FT cells were transiently transfected with V5-tagged Hippo pathway core molecules (NF2, KIBRA, AMOT, AMOTL1, MST1/2, LATS1/2, SAV1, YAP1 and 14-3-3 η) and cell lysates were immunoprecipitated by an anti-CADM1 antibody. The co-precipitation of CADM1 with these molecules was detected by western blotting with an anti-V5 antibody. Red arrows indicate positive signals. Co-precipitation experiments were performed at least twice

was coprecipitated with NF2, KIBRA, SAV1, MST1/2, LATS1/2, AMOTL1 and 14-3-3 η , but not with YAP1 or AMOT (Figure 2). These results suggest that CADM1 forms complexes with Hippo pathway core molecules at the cell membrane. We also confirmed that endogenous CADM1 and LATS2 interacted in the lung adenocarcinoma cell line H1838 using an immunoprecipitation assay (Figure S3). We speculated that CADM1 recruits the Hippo pathway core kinases MST1/2 and LATS1/2 to the cell membrane through scaffold protein complexes containing NF2 and KIBRA, which activates a kinase cascade reaction.

3.4 | Immunohistochemical expression of LATS2 and CADM1 in primary lung adenocarcinoma tissues and their relationships with histological types, clinicopathological factors, and disease-free survival

The junctional localization of LATS1/2 plays an important role in the regulation of the Hippo pathway. LATS1/2 has been shown to directly phosphorylate YAP1,^{20,21} and the recruitment of LATS1/2 to the cell membrane is needed to promote the phosphorylation of

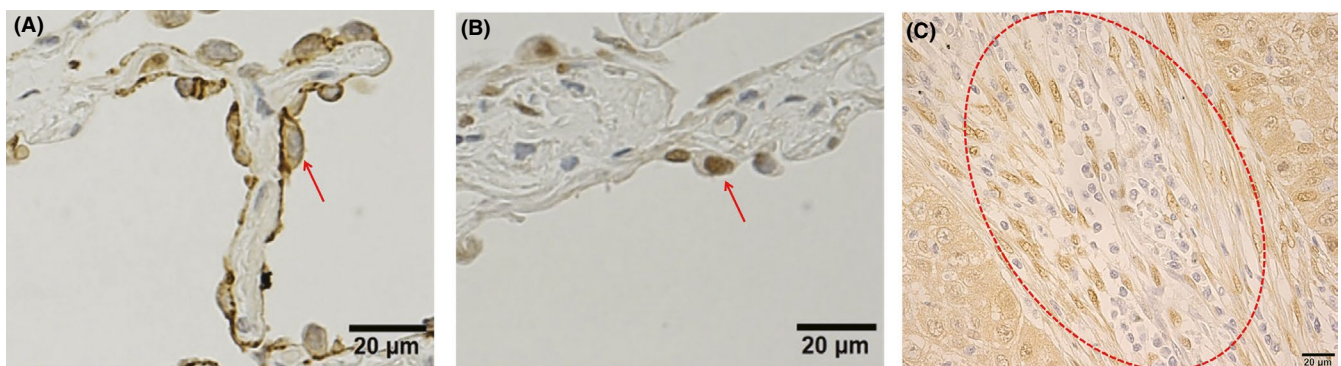


FIGURE 3 A, Reactive type II pneumocytes as an internal positive control for LATS2, showing membranous LATS2-positive staining. The red arrow indicates a reactive type II pneumocyte. B, Reactive type II pneumocytes as an internal positive control for YAP1, showing nuclear YAP1-positive staining. The red arrow indicates a reactive type II pneumocyte. C, Fibroblasts as an internal positive control for YAP1, showing nuclear and cytoplasmic YAP1-positive staining. A red circle surrounds fibroblasts

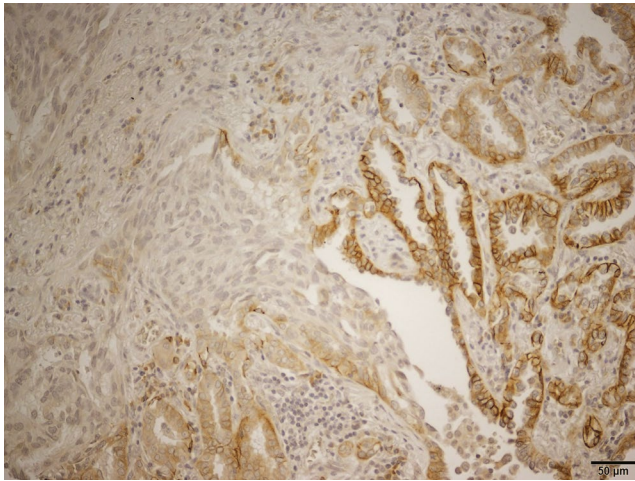


FIGURE 4 Typical expression pattern of LATS2 in invasive lung adenocarcinoma. LATS2 showed a heterogeneous staining pattern, typically demonstrating strong membranous-positive staining in lepidic growth (adenocarcinoma *in situ*) components (right side), while losing membranous staining in invasive components (left side)

TABLE 1 Relationship between membranous CADM1 and LATS2 expression levels in 145 cases

	Membranous CADM1 expression		P-value
	Positive	Negative	
Membranous LATS2 expression			
Positive	58	9	<0.0001
Negative	36	42	

LATS1/2.²² However, the membranous expression of LATS1/2 in primary lung tumors has not yet been investigated.

To confirm whether CADM1 forms a complex with Hippo pathway core molecules in primary lung adenocarcinomas, we selected LATS2 as a representative of Hippo pathway core kinases interacting with CADM1, and examined the immunohistochemical expression of LATS2, particularly in the cell membrane, as well as its relationships with: (i) CADM1 expression; (ii) histopathological subtypes; (iii) clinicopathological factors; and (iv) disease-free survival using the TMA sections of 145 primary lung adenocarcinoma cases.

Reactive type II pneumocytes constantly stained positive in the membrane for LATS2 (Figure 3A) and were weakly positive in the membrane for CADM1, as previously reported,⁶ and, thus, served as excellent internal positive controls.

Among 145 cases, 66 (46%) were judged to show the membranous expression of LATS2, 35 (24%) cytoplasmic expression, but no membranous expression of LATS2, and 44 (30%) the completely negative expression of LATS2, while 92 cases (63%) were judged as showing the membranous expression of CADM1 and 53 (37%) the negative expression of membranous CADM1.

LATS2 and CADM1 showed similar expression patterns: LATS2, similar to CADM1 as reported in our previous study,⁶ showed a heterogeneous staining pattern, typically demonstrating strong membranous positive staining in lepidic growth (adenocarcinoma *in situ*) components, while losing membranous staining in the invasive component (Figure 4). Table 1 shows that LATS2 was significantly co-expressed with CADM1 in the membranes of primary lung adenocarcinomas ($P < 0.0001$).

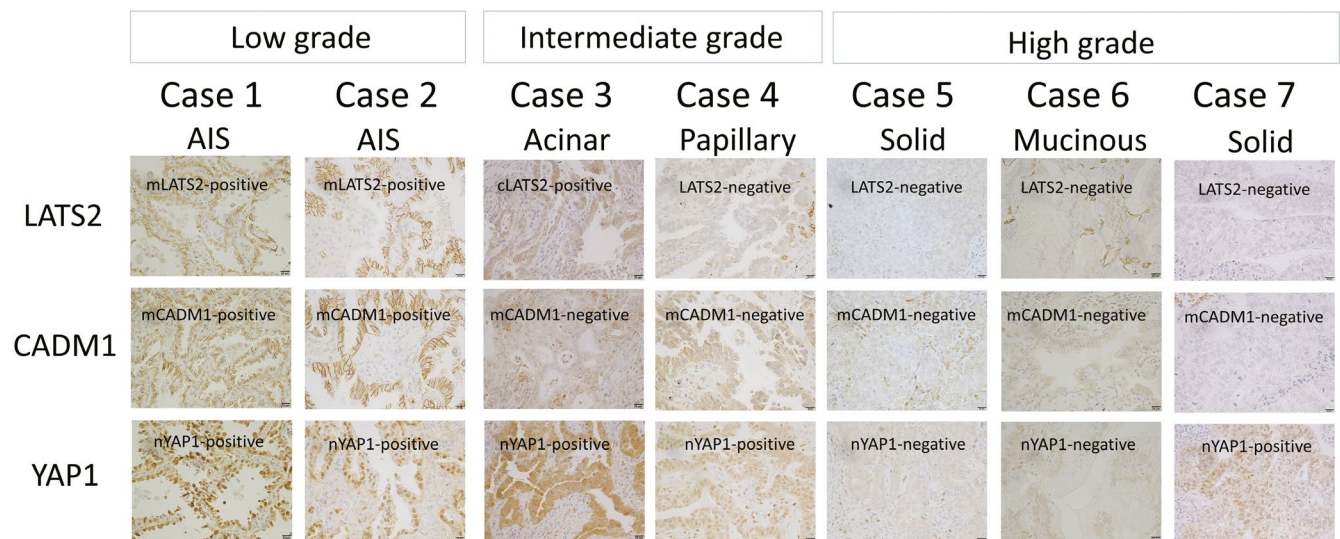


FIGURE 5 Staining of sections from 7 cases, including 2 representative cases of low-grade adenocarcinomas (2 non-mucinous adenocarcinomas *in situ* [AIS]) (cases 1 and 2), 2 representative cases of intermediate-grade adenocarcinomas (1 acinar adenocarcinoma and 1 papillary adenocarcinoma) (cases 3 and 4), and 3 representative cases of high-grade adenocarcinomas (2 solid adenocarcinomas and 1 invasive mucinous adenocarcinoma) (cases 5, 6 and 7) for LATS2, CADM1 and YAP1. mLATS2-positive mean membranous LATS2-positive, cLATS2-positive; cytoplasmic LATS2-positive, mCADM1-positive/negative; membranous CADM1-positive/negative, and nYAP1-positive/negative; nuclear YAP1-positive/negative

TABLE 2 Comparison of expression levels of (i) membranous CADM1, (ii) membranous LATS2, (iii) nuclear YAP1 and (iv) cytoplasmic YAP1 with histological grades among 145 cases

	Histological grades			P-value
	Low	Intermediate	High	
Membranous CADM1				
Positive	20	61	13	<0.0001
Negative	2	30	19	
Membranous LATS2				
Positive	22	44	1	<0.0001
Negative	0	47	31	
Nuclear YAP1				
Positive	19	37	6	<0.0001
Negative	3	54	26	
Cytoplasmic YAP1				
Positive	21	75	18	0.0023
Negative	1	16	14	

Non-mucinous adenocarcinoma in situ (low-grade subtype) frequently showed the strong co-expression of membranous LATS2 and CADM1 (Figure 5 cases 1 and 2), while papillary or acinar adenocarcinomas, intermediate-grade subtypes, gradually showed the loss of membranous LATS2 and CADM1 expression, sometimes retaining the cytoplasmic expression of LATS2 (Figure 5 cases 3 and 4), and solid adenocarcinoma and invasive mucinous adenocarcinoma, high-grade subtypes, frequently showed completely negative staining for both LATS2 and CADM1 (Figure 5 cases 5, 6 and 7). Table 2 shows that the strong expression of membranous CADM1 and LATS2 correlated with a lower histological grade ($P < 0.0001$, $P < 0.0001$, respectively).

Tables 3 and 4 show the relationships between membranous LATS2 and CADM1 expression levels and clinicopathological factors, respectively. The loss of membranous CADM1 and LATS2 expression correlated with advanced pathological stages, advanced pT stages, lymph node metastasis, lymphatic invasion, vessel invasion, pleural invasion and tumor size (Tables 3 and 4). These results supported the roles of CADM1 and LATS2 as critical tumor suppressors in lung adenocarcinomas.

Figure 6A,B shows disease-free survival curves based on CADM1 and LATS2 expression patterns, respectively. Membranous CADM1-positive cases ($n = 92$) showed a significantly better prognosis than membranous CADM1-negative cases ($n = 50$) in Figure 6A ($P = 0.0040$). In Figure 6B, membranous LATS2-positive cases ($n = 66$) showed the best prognosis (5-year disease-free survival rate = 79.8%), whereas LATS2-negative cases ($n = 41$) had the worst prognosis (5-year disease-free survival rate = 48.7%). The 5-year disease-free-survival rate of cytoplasmic LATS2-positive cases ($n = 35$) was 67.0%.

Among membranous CADM1-positive cases ($n = 92$), membranous LATS2-positive cases ($n = 57$) showed the best prognosis (5-year disease-free survival rate = 83.8%), cytoplasmic LATS2-positive cases ($n = 23$) an intermediate prognosis (5-year disease-free survival

TABLE 3 Relationships between membranous CADM1 expression levels and clinicopathological factors in 145 primary lung adenocarcinoma cases

	Membranous CADM1 expression			P-value
	Positive	Negative		
Age				
65>	38	23		0.5863
65≤	56	28		
Sex				
Male	44	34		0.0220
Female	50	17		
Pathological stage ^a				
Stage 0-I	78	29		0.0011
Stage II-IV	16	21		
T-stage				
Tis, T1	55	13		0.0001
T2, T3, T4	39	38		
Nodal involvement ^b				
Positive	16	18		0.0084
Negative	76	30		
Lymphatic invasion				
Positive	14	19		0.0022
Negative	80	32		
Vessel invasion				
Positive	26	29		0.0005
Negative	68	22		
Pleural invasion				
Positive	32	33		0.0004
Negative	62	18		
Tumor size				
3 cm>	77	28		0.0005
3 cm≤	17	32		
Pulmonary metastasis				
Positive	4	7		0.0397
Negative	90	44		
Smoking index ^c				
500>	57	21		0.0271
500≤	33	27		
EGFR mutations ^d				
Positive	35	12		0.0045
Negative	31	34		

^aThe stages of 3 cases were unknown (2 were more than Stage I).

^bThe presence or absence of nodal involvement was unknown in 5 cases.

^cThe smoking index was unknown in 7 cases.

^dThe presence or absence of EGFR mutations was unknown in 33 cases.

rate = 68.1%) and LATS2-negative cases ($n = 12$) the worst prognosis (4-year disease-free survival rate = 48.5%) (in Figure 6C), while among membranous CADM1-negative cases ($n = 50$), disease-free

TABLE 4 Relationships between membranous LATS2 expression levels and clinicopathological factors in 145 primary lung adenocarcinoma cases

	Membranous LATS2 expression		P-value
	Positive	Negative	
Age			
65>	41	43	0.4607
65≤	26	35	
Sex			
Male	28	50	0.0072
Female	39	28	
Pathological stage ^a			
Stage 0-I	57	50	0.0058
Stage II-IV	10	27	
T-stage			
Tis, T1	44	24	<0.0001
T2, T3, T4	23	54	
Nodal involvement ^b			
Positive	10	24	0.0173
Negative	56	50	
Lymphatic invasion			
Positive	7	26	0.0010
Negative	60	52	
Vessel invasion			
Positive	10	45	<0.0001
Negative	57	33	
Pleural invasion			
Positive	20	45	0.0008
Negative	47	33	
Tumor size			
3 cm>	59	46	<0.0001
3 cm≤	8	32	
Pulmonary metastasis			
Positive	6	5	0.5639
Negative	61	73	
Smoking index ^c			
500>	46	32	0.0014
500≤	19	41	
EGFR mutations ^d			
Positive	30	17	0.0001
Negative	18	47	

^aThe stages of 3 cases were unknown (2 were more than Stage I).

^bThe presence or absence of nodal involvement was unknown in 5 cases.

^cThe smoking index was unknown in 7 cases.

^dThe presence or absence of EGFR mutations was unknown in 33 cases.

survival was similar for membranous LATS2-positive cases (n = 9), cytoplasmic LATS2-positive cases (n = 12) and LATS2-negative cases (n = 29) (5-year disease-free survival rate = 55.6%, 65.6% and 50.2%,

respectively) (in Figure 6D). These results suggest that LATS2 exhibits tumor suppressor activity preferentially in the presence of CADM1.

3.5 | Immunohistochemical expression of YAP1 in primary lung adenocarcinoma tissues

YAP1 was positive in the nucleus and cytoplasm of fibroblasts, and also positive in the nucleus of reactive type II pneumocytes (Figure 3B,C), and, thus, served as an excellent internal positive control.

Most low-grade and intermediate-grade lung adenocarcinomas showed high expression levels of nuclear and/or cytoplasmic YAP1 (Figure 5 cases 1-4). Non-mucinous adenocarcinoma in situ (low-grade subtype) frequently showed high expression levels of nuclear YAP1 (Figure 5 cases 1 and 2), while solid adenocarcinoma and invasive mucinous adenocarcinoma (high-grade subtypes) frequently showed negative staining for nuclear and cytoplasmic YAP1 (Figure 5 cases 5 and 6). Table 2 shows that high expression levels of nuclear and cytoplasmic YAP1 correlated with a lower histological grade ($P < 0.0001$, $P = 0.0023$, respectively). These results were consistent with previous findings showing that nuclear YAP1 expression was typically observed in well-differentiated pulmonary adenocarcinoma.²³ However, a small number of solid adenocarcinoma cases were positive for nuclear YAP1 (Figure 5 case 7).

3.6 | Disease-free survival curves based on expression patterns of membranous CADM1, membranous LATS2 and nuclear YAP1

Disease-free survival was similar for nuclear YAP1-positive cases (n = 60) and nuclear YAP1-negative cases (n = 82) in the present study (Figure 7A). We then subdivided lung adenocarcinoma cases into 8 patterns depending on membranous CADM1 (mCADM1), membranous LATS2 (mLATS2) and nuclear YAP1 (nYAP1) expression levels, and performed a disease-free survival analysis on the 8 patterns. The results obtained are shown in Figure 7B. The 8 patterns were classified into 3 groups: a favorable prognosis group (mCADM1+/mLATS2+/nYAP1+ and mCADM1+/mLATS2+/nYAP1-), a poor prognosis group (mCADM1-/mLATS2-/nYAP1+) and an intermediate prognosis group (the other patterns) (Figure 7B).

Membranous CADM1-positive and LATS2-positive cases both showed the best prognosis, regardless of whether nuclear YAP1 was present or absent (5-year disease-free survival rates = 83.7 and 83.1%, respectively). However, nuclear YAP1-positive cases with the loss of membranous CADM1 and LATS2 expression showed the worst prognosis (5-year disease-free-survival rate = 33.3%).

In the present study, non-mucinous adenocarcinoma in situ, a representative of the terminal respiratory unit type (TRU type) with thyroid transcription factor 1 (TTF1) expression and an extremely good prognosis, retained the same staining pattern of CADM1, LATS2 and YAP1 as type II pneumocytes; namely, membranous CADM1 and LATS2 co-expression and nuclear YAP1 expression.

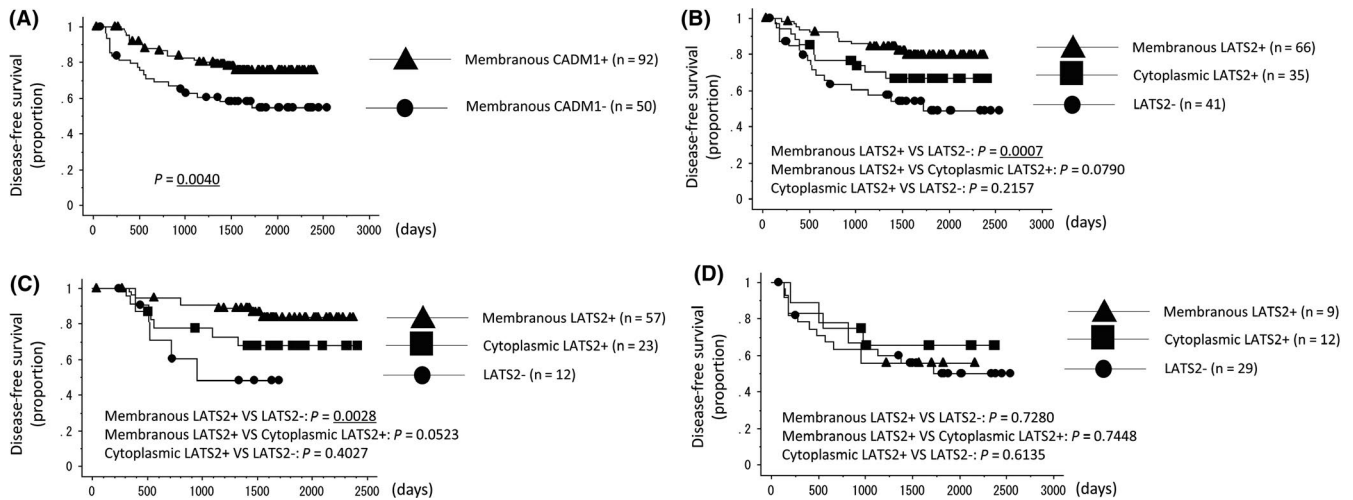


FIGURE 6 A, Disease-free survival curves according to membranous CADM1 expression levels among 142 cases. Patients were classified into 2 groups: a membranous CADM1-positive group ($n = 92$) and CADM1-negative group ($n = 50$). B, Disease-free survival curves according to LATS2 expression patterns among 142 cases. Patients were classified into 3 groups: membranous LATS2-positive cases ($n = 66$), cytoplasmic LATS2-positive cases ($n = 35$), and LATS2-negative cases ($n = 41$). C, Disease-free survival curves according to LATS2 expression patterns among membranous CADM1-positive cases ($n = 92$). Patients were classified into 3 groups: membranous LATS2-positive cases ($n = 57$), cytoplasmic LATS2-positive cases ($n = 23$) and LATS2-negative cases ($n = 12$). D, Disease-free survival curves according to LATS2 expression patterns among membranous CADM1-negative cases ($n = 50$). Patients were classified into 3 groups: membranous LATS2-positive cases ($n = 9$), cytoplasmic LATS2-positive cases ($n = 12$), and LATS2-negative cases ($n = 29$)

Non-mucinous adenocarcinoma in situ showed the replacement growth of alveolar-lining epithelial cells without invasion or solid proliferation; therefore, we speculated that contact inhibition through the Hippo pathway is not required in non-mucinous adenocarcinoma in situ, even with the co-expression of CADM1 and LATS2.

Based on these results, we focused on invasive adenocarcinoma cases ($n = 120$) and performed a disease-free survival analysis depending on the expression levels of: (i) CADM1 and nuclear YAP1; and (ii) membranous LATS2 and nuclear YAP1. The results obtained are shown in Figure S4. In invasive adenocarcinoma cases, the prognosis of nuclear YAP1-positive cases with membranous LATS2/CADM1 expression was significantly better than that of nuclear YAP1-positive cases without membranous LATS2/CADM1 expression (Figure S4).

These results suggest that the oncogenic role of nuclear YAP1 was inhibited by the co-expression of membranous CADM1 and LATS2.

4 | DISCUSSION

CADM1 was originally identified as a tumor suppressor that encodes an immunoglobulin superfamily cell adhesion molecule (IgCAM). CADM1 suppresses the proliferation of the subcutaneous tumors of lung adenocarcinoma cell lines by inducing apoptosis^{3,4,8}; however, the underlying molecular mechanisms have not been elucidated in sufficient detail. The Hippo pathway is emerging as a tumor suppressor pathway in the contact inhibition of proliferation, and to the best of our knowledge, this is the first study

to show that CADM1 is involved in the regulation of the Hippo pathway through cell-cell contact.

In *Drosophila*, Echinoid, an IgCAM member, has been shown to facilitate Hippo (MST1/2 in mammals) activation and subsequent Yorkie (YAP1) phosphorylation by interacting with multiple components of the Hippo pathway, including the scaffold proteins Salvador (SAV1), Merlin (NF2), Expanded (FRMD6) and KIBRA.¹¹ Salvador (SAV1) is a key molecule among these scaffold proteins; SAV1 localizes to the cell membrane through an interaction with Echinoid, and then recruits Hippo to the cell-cell junction.²⁴ Merlin directly binds and recruits Warts (LATS1/2) to the plasma membrane, while membrane recruitment promotes Warts phosphorylation by the Hippo-Salvador kinase complex.²² In the present study, we found that CADM1 formed complexes with multiple Hippo pathway core molecules: MST1/2, LATS1/2, SAV1, NF2 and KIBRA, similar to Echinoid. Therefore, we speculate that CADM1 functions as the human counterpart of Echinoid; it recruits the MST1/2 and LATS1/2 kinases to the cell membrane by forming scaffold protein complexes through its binding with SAV1 in cell junctions upon cell-cell contact, initiating an MST1/2-LATS1/2-YAP1 phosphorylation cascade. In addition, our IP assay revealed that CADM1 did not associate with YAP1, suggesting that YAP1 is not recruited to the cell membrane by CADM1. We speculate that LATS1/2 moves to the cytosol or nucleus, at which it directly phosphorylates YAP1 after being phosphorylated in the cell membrane.

The relationship between CADM1 and Hippo pathway core kinases at the cell membrane, and its tumor suppressive role were confirmed by immunohistochemical findings showing that the co-expression of CADM1 and LATS2 in the cell membrane was significantly frequent in the histologically low-grade cases with a better

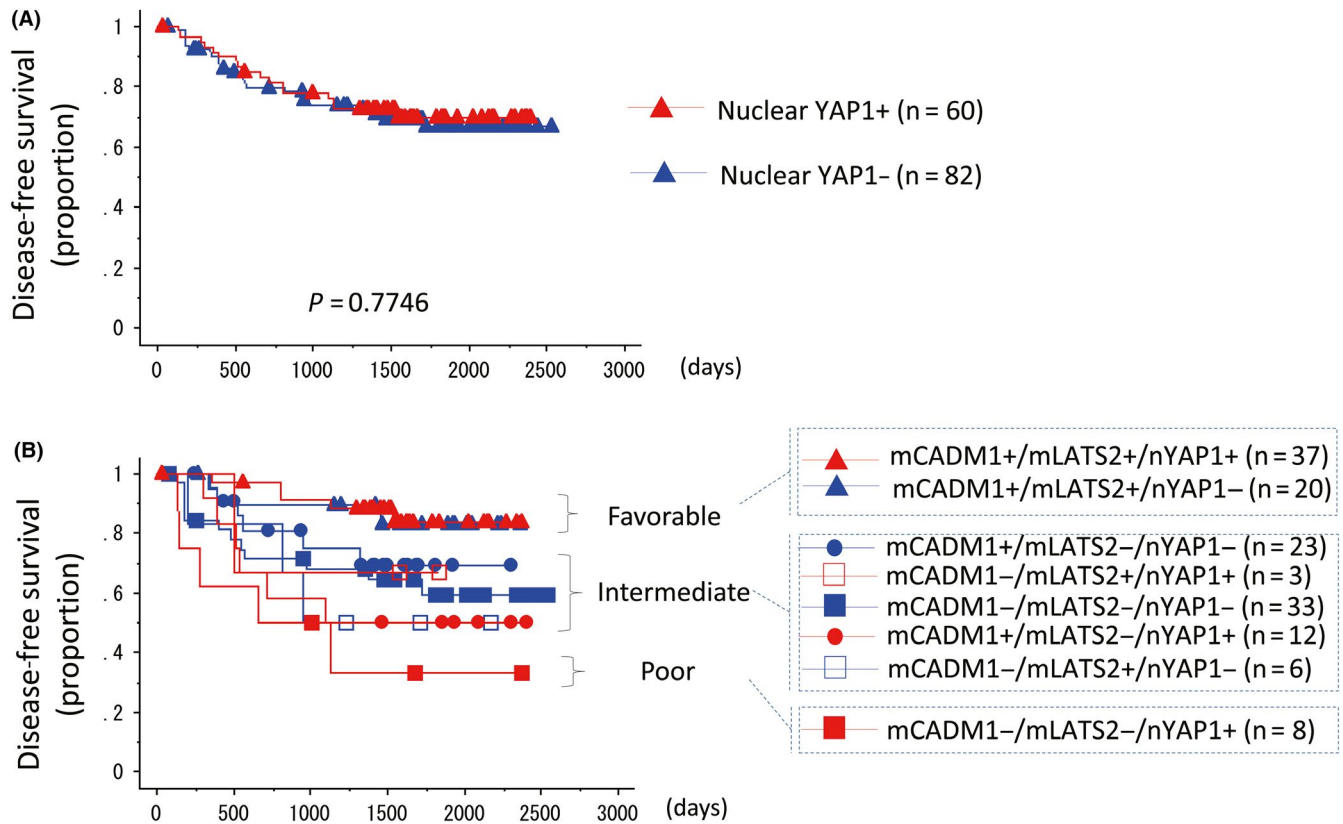


FIGURE 7 A, Disease-free survival curves according to nuclear YAP1 expression levels among 142 cases. Patients were classified into 2 groups: a nuclear YAP1-positive group (n = 60) and YAP1-negative group (n = 50). B, Disease-free survival curves according to membranous CADM1 (mCADM1), membranous LATS2 (mLATS2), and nuclear YAP1 (nYAP1) expression levels among 142 cases. Patients were classified into 8 patterns and subdivided into 3 groups: a favorable prognosis group (mCADM1+/mLATS2+/nYAP1+ (n = 37), and mCADM1+/mLATS2+/nYAP1- (n = 20)), intermediate prognosis group (mCADM1+/mLATS2-/nYAP1- (n = 23), mCADM1-/mLATS2+/nYAP1+ (n = 3), mCADM1-/mLATS2-/nYAP1- (n = 33), mCADM1+/mLATS2-/nYAP1+ (n = 12), and mCADM1-/mLATS2+/nYAP1- (n = 6)), and poor prognosis group (mCADM1-/mLATS2-/nYAP1+ (n = 8))

prognosis, and that nuclear YAP1-positive cases with the co-expression of CADM1 and LATS2 in the membrane showed a favorable prognosis, while nuclear YAP1-positive cases with negative expression for CADM1 and LATS2 had the worst prognosis. These results suggest that CADM1 suppresses the progression of lung adenocarcinoma by inactivating YAP1 in combination with LATS2, as observed in cell experiments.

However, the tumor suppressor activity of CADM1 does not necessarily depend on YAP1 because the re-expression of CADM1 was shown to strongly induce apoptosis in the A549 lung adenocarcinoma cell line, which expresses a very low level of YAP1.^{7,25} Further analyses are required to elucidate the molecular mechanisms responsible for the YAP1-independent tumor suppressor activity of CADM1.

Nuclear YAP1 was previously reported to correlate with a worse prognosis in non-small cell lung cancer (non-SCLC).²⁵ However, nuclear YAP1 expression was frequently found in non-mucinous adenocarcinoma in situ (low-grade subtype) and reactive type II pneumocytes in the present study. YAP1 has been shown to inhibit the squamous differentiation of LKB1-deficient lung adenocarcinomas.²⁶ We previously reported that the loss of YAP1 correlated

with the neuroendocrine differentiation of lung tumors,²⁷ demonstrating that SCLC with adenocarcinoma components frequently showed the loss of YAP1 in the components of SCLC and strong positivity in adenocarcinoma components.²⁷ Otsubo et al²⁸ reported the involvement of the MOB1-YAP1/TAZ-NKX2.1 signal in bronchoalveolar cell differentiation. Based on these findings, we speculate that YAP1 functions as a key regulator of differentiation, and its oncogenic activities, even with nuclear-positive staining, may be controlled in the presence of CADM1 interacting with Hippo pathway core kinases.

Our IP assay also revealed that CADM1 associated with AMOTL1 and 14-3-3 η , suggesting that the relationships between CADM1, AMOTL1 and 14-3-3 η are involved in the cytoplasmic retention of YAP1. CADM1 may still form a complex with HER3,²⁹ suggesting that CADM1 induces Hippo pathway signaling by inhibiting HER3/HER2-RAS signaling; these may be the mechanisms by which CADM1 regulates YAP1 and will be the focus of future research.

In summary, by associating with multiple components of the Hippo pathway in membranes, CADM1 potentially functions as a molecular scaffold to facilitate Hippo pathway activation and YAP1 phosphorylation.

ACKNOWLEDGMENTS

We thank Takuya Tabuchi and Yutaro Shiraishi for their technical assistance, and also acknowledge the IMSUT FACS Core laboratory for their assistance with the flow cytometric analysis.

DISCLOSURE

The authors have no conflict of interest.

ORCID

Daisuke Matsubara  <https://orcid.org/0000-0002-6233-6840>

Yoshinori Murakami  <https://orcid.org/0000-0002-2826-4396>

REFERENCES

1. Statistics and Information Department. *Vital Statistics, 2000*. Tokyo, Japan: Ministry of Health, Labor and Welfare; 2001.
2. Jemal A, Siegel R, Ward E, et al. Cancer statistics, 2006. *CA Cancer J Clin*. 2006;56:106-130.
3. Kuramochi M, Fukuhara H, Nobukuni T, et al. TSLC1 is a tumor-suppressor gene in human non-small-cell lung cancer. *Nat Genet*. 2001;27:427-430.
4. Murakami Y. Functional cloning of a tumor suppressor gene, TSLC1, in human non-small cell lung cancer. *Oncogene*. 2002;21:6936-6948.
5. Masuda M, Yageta M, Fukuhara H, et al. The tumor suppressor protein TSLC1 is involved in cell-cell adhesion. *J Biol Chem*. 2002;277:31014-31019.
6. Goto A, Niki T, Chi-pin L, et al. Loss of TSLC1 expression in lung adenocarcinoma: relationships with histological subtypes, sex and prognostic significance. *Cancer Sci*. 2005;96:480-486.
7. Mao X, Seidlitz E, Truant R, Hitt M, Ghosh HP. Re-expression of TSLC1 in a non-small-cell lung cancer cell line induces apoptosis and inhibits tumor growth. *Oncogene*. 2004;23:5632-5642.
8. Mao X, Seidlitz E, Ghosh K, Murakami Y, Ghosh HP. The cytoplasmic domain is critical to the tumor suppressor activity of TSLC1 in non-small cell lung cancer. *Cancer Res*. 2003;63:7979-7985.
9. Harvey KF, Zhang X, Thomas DM. The Hippo pathway and human cancer. *Nat Rev Cancer*. 2013;13:246-257.
10. Zhao B, Tumaneng K, Guan KL. The Hippo pathway in organ size control, tissue regeneration and stem cell self-renewal. *Nat Cell Biol*. 2011;13:877-883.
11. Yue T, Tian A, Jiang J. The cell adhesion molecule echinoid functions as a tumor suppressor and upstream regulator of the Hippo signaling pathway. *Dev Cell*. 2012;22:255-267.
12. Ito T, Williams-Nate Y, Iwai M, et al. Transcriptional regulation of the CADM1 gene by retinoic acid during the neural differentiation of murine embryonal carcinoma P19 cells. *Genes Cells*. 2011;16:791-802.
13. Morgenstern JP, Land H. Advanced mammalian gene transfer: high titre retroviral vectors with multiple drug selection markers and a complementary helper-free packaging cell line. *Nucleic Acids Res*. 1990;18:3587-3596.
14. Kitamura T, Koshino Y, Shibata F, et al. Retrovirus-mediated gene transfer and expression cloning: powerful tools in functional genomics. *Exp Hematol*. 2003;31:1007-1014.

15. Ito T, Kasai Y, Kumagai Y, et al. Quantitative analysis of interaction between CADM1 and its binding cell-surface proteins using surface plasmon resonance imaging. *Front Cell Dev Biol*. 2018;6:86.
16. UICC International Union Against Cancer. *TNM Classification of Malignant Tumours*, 7th edn. New York, NY: Wiley Blackwell; 2009.
17. Yoshizawa A, Motoi N, Riely GJ, et al. Impact of proposed IASLC/ATS/ERS classification of lung adenocarcinoma: prognostic subgroups and implications for further revision of staging based on analysis of 514 stage I cases. *Mod Pathol*. 2011;24:653-664.
18. Zhao B, Wei X, Li W, et al. Inactivation of YAP oncoprotein by the Hippo pathway is involved in cell contact inhibition and tissue growth control. *Genes Dev*. 2007;21:2747-2761.
19. Zhao B, Li L, Lei Q, Guan KL. The Hippo-YAP pathway in organ size control and tumorigenesis: an updated version. *Genes Dev*. 2010;24:862-874.
20. Dong J, Feldmann G, Huang J, et al. Elucidation of a universal size-control mechanism in Drosophila and mammals. *Cell*. 2007;130:1120-1133.
21. Oh H, Irvine KD. In vivo analysis of Yorkie phosphorylation sites. *Oncogene*. 2009;28:1916-1927.
22. Yin F, Yu J, Zheng Y, Chen Q, Zhang N, Pan D. Spatial organization of Hippo signaling at the plasma membrane mediated by the tumor suppressor Merlin/NF2. *Cell*. 2013;154:1342-1355.
23. Kim MH, Kim YK, Shin DH, et al. Yes associated protein is a poor prognostic factor in well-differentiated lung adenocarcinoma. *Int J Clin Exp Pathol*. 2015;8:15933-15939.
24. Su T, Ludwig MZ, Xu J, Fehon RG. Kibra and merlin activate the hippo pathway spatially distinct from and independent of expanded. *Dev Cell*. 2017;40:478-490.
25. Wang Y, Dong Q, Zhang Q, Li Z, Wang E, Qiu X. Overexpression of yes-associated protein contributes to progression and poor prognosis of non-small-cell lung cancer. *Cancer Sci*. 2010;101:1279-1285.
26. Gao Y, Zhang W, Han X, et al. YAP inhibits squamous transdifferentiation of Lkb1-deficient lung adenocarcinoma through ZEB2-dependent DNp63 repression. *Nat Commun*. 2014;5:4629.
27. Ito T, Matsubara D, Tanaka I, et al. Loss of YAP 1 defines neuroendocrine differentiation of lung tumors. *Cancer Sci*. 2016;107:1527-1538.
28. Otsubo K, Goto H, Nishio M, et al. The MOB1-YAP1/TAZ-NKX2.1 axis controls bronchioalveolar cell differentiation, adhesion and tumour formation. *Oncogene*. 2017;36:4201-4211.
29. Kawano S, Ikeda W, Kishimoto M, Ogita H, Takai Y. Silencing of ErbB3/ErbB2 signaling by immunoglobulin-like Necl-2. *J Biol Chem*. 2009;284:23793-23805.

SUPPORTING INFORMATION

Additional supporting information may be found online in the Supporting Information section at the end of the article.

How to cite this article: Ito T, Nakamura A, Tanaka I, et al. CADM1 associates with Hippo pathway core kinases; membranous co-expression of CADM1 and LATS2 in lung tumors predicts good prognosis. *Cancer Sci*. 2019;110:2284-2295. <https://doi.org/10.1111/cas.14040>